Automatic Atherosclerotic Heart Disease Detection in Intracoronary Optical Coherence Tomography Images

Mengdi Xu, Jun Cheng, Damon Wing Kee Wong, Akira Taruya, Atsushi Tanaka and Jiang Liu

***Abstract*— Intracoronary optical coherence tomography (OCT) is a new invasive imaging system which produces high-resolution images of coronary arteries. Preliminary data suggests that the atherosclerotic disease can be detected from the intracoronary OCT images. However, manual assessment of the intracoronary OCT images is time-consuming and subjective. In this work, we present an automatic atherosclerotic disease detection system on intracoronary OCT images. In the system, a preprocessing scheme is first applied to remove speckle noise and artifacts caused by catheter. Intensity, Histograms of Oriented Gradients (HOG), and Local Binary Patterns (LBP) are then extracted to represent the OCT image. Finally a linear SVM classifier is employed to detect the unhealthy subject. Four-fold cross-validation process is conducted to evaluate the proposed system; and a dataset with 200 images from healthy subjects and 200 images from unhealthy subjects is built to evaluate the system. The mean accuracy is 0.90 and standard deviation is 0.0427, which indicates that the proposed system is accurate and stable.**

I. INTRODUCTION

Coronary artery disease, also known as atherosclerotic heart disease, is the most common type of heart disease and cause of heart attacks. The disease is caused by plaque building up along the inner walls of the arteries of the heart, which narrows the arteries and reduces blood flow to the heart. Fig. 1 shows the timeline of atherosclerosis. With the progress of atherosclerosis, the stages are normal, pathological intimal thickening (PIT), stable plaque, atherosclerotic plaque, and rupture. There is growing interest in the possibility that identification and treatment of vulnerable plaques and vulnerable patients can enhance the progress made against coronary artery diseases.

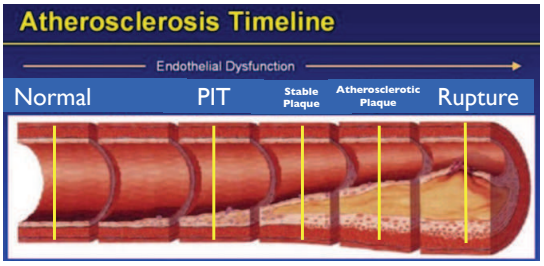

Fig. 1. Atherosclerosis timeline.

Mengdi Xu, Jun Cheng, Damon Wing Kee Wong and Jiang Liu are with the Institute for Infocomm Research, A*STAR, Singapore (phone: (065)6408-2550; fax: (065)6776-1378); email: xumd@i2r.a-star.edu.sg).

Akira Taruya and Atsushi Tanaka are with the Cardiovascular Division, Wakayama Medical University, Wakayama, Japan (email: a-tanaka@wakayama-med.ac.jp).

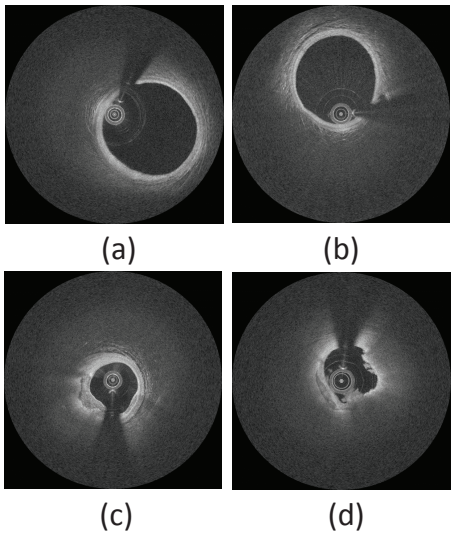

Fig. 2. Some OCT images in our dataset. (a) and (b) are images from healthy subjects. (c) shows image from subject with atherosclerotic plaque, and (d) shows image from subject with ruptured plaque. Both (c) and (d) are images from unhealthy subjects.

Recently, intracoronary Optical Coherence Tomography (OCT) [1][2] has emerged as one of the most promising intracoronary diagnostic tools with a resolution 15 um compared with 150 um of intravascular ultrasound system (IVUS), allowing a level of detail never reached before. The OCT acquisition has already been proved to be safe, effective, and highly reproducible [1]. Previous study suggests that OCT could help to characterize the appearance of vulnerable plaques [2]. However, manual assessment of the intracoronary OCT images is time-consuming and subjective, thus it is necessary to build an automatic vulnerable plaques characterization system. Instead of characterizing the appearance of vulnerable plaques, we propose a preliminary system which classifies unhealthy subjects from healthy subjects in intracoronary OCT images.

Most existing automatic OCT systems focused on vessel lumen segmentation or stent strut detection problems. Tsantis *et al.* [3] presented an automatic vessel lumen segmentation method based on Markov Random Field (MRF) model. Some researchers focused on other problems such as calcified plaque detection. Athanasious *et al.* [4] proposed an automatic method for detecting calcified plaque in OCT images. The proposed method was fully automated but only calcified plaque region was detected. Athanasious *et al.* [5] also introduced a semi-automated plaque characterization

978-1-4244-7929-0/14/$26.00 ©2014 IEEE

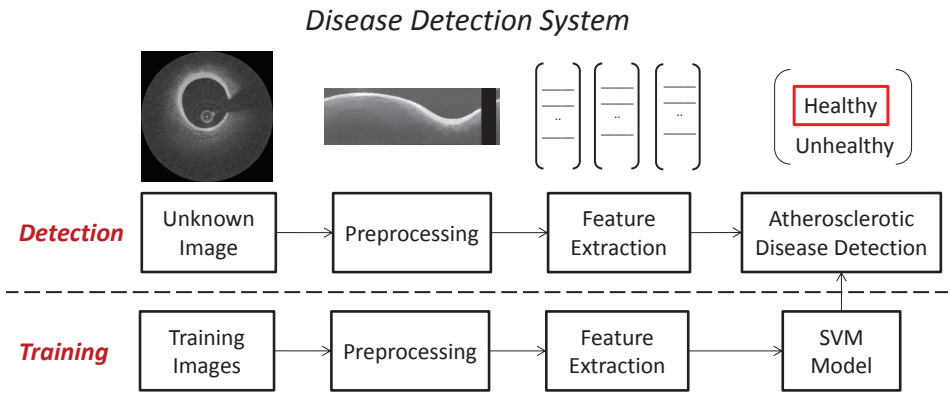

Fig. 3. Framework of our proposed system. The detection system includes a preprocessing step to remove noise and artifacts; a feature extraction step to extract representative features; and a detection step to decide whether the input image is from healthy or unhealthy subject by utilizing the model trained in the training process. Similarly, training process includes a preprocessing step, a feature extraction step, and a step to train linear SVM model. The detection process and training process have the same preprocessing and feature extraction procedure.

method in optical coherence tomography images. The plaque area (Region of Interest) was selected manually by users and the plaques were classified to four plaque types. The overall classification accuracy was 80.41%. However, this plaque characterization method was semi-automated since the plaque area was selected by users manually; and it classified pixels instead of the entire images.

In this work, we propose an automatic atherosclerotic heart disease detection system which accurately classifies image to healthy and unhealthy subjects by utilizing appearance features. The proposed system includes three steps: preprocessing, feature extraction, and detection (classification) using SVM model. The SVM model is built by the training process. In this process, the training images are processed using preprocessing scheme, feature extraction scheme, and a linear SVM model is built for diseased subject detection. Four-fold cross-validation is conducted to evaluate the system. A dataset with 400 annotated OCT images (200 images from healthy subjects and 200 images from unhealthy subjects) is built for the evaluation process. Fig. 2 shows some images in the dataset. Here healthy subject means patient with normal heart and blood vessel (Normal in Fig. 1), unhealthy subject means patient with non-normal heart and blood vessels (PIT, stable plaque, atherosclerotic plaque, and ruptured plaque in Fig. 1). Evaluation results show that the proposed system is accurate and stable.

II. METHODOLOGY

This section introduces technical details of the three main steps in our system: preprocessing to remove noise and artifacts, feature extraction to represent the OCT images, and disease detection to decide whether the input unknown OCT image is from healthy or unhealthy subject. Fig. 3 shows our framework. Both detection and training process have the same preprocessing and feature extraction scheme.

A. Preprocessing

We apply the following procedure to remove noise and artifacts of the input OCT images.

- Remove the speckle noise using detail preserving anisotropic diffusion (DPAD) method [6].
- Convert the image to polar coordinates. One may notice that the catheter pixels are transferred from circle to line after the transformation thus can be removed easily by deleting the top N rows of the polar coordinates image. Noted that all the input OCT images are square images, here N is set to be $0.125 * W/2$ empirically. W is the width of the input OCT image.
- Remove other artifacts by deleting the black sector which caused by occlusion. The occluded region is shown in Fig. 4. The area within the red lines (acute angle) is the black sector area. To remove it, we slide a box over the polar image from left to right and calculate the mean intensity within the box region. The place where the smallest mean intensity value appears is sector location. The height of the box is the height of the denoised image and the width is set to be 30 empirically. Fig. 5 shows the details.

Fig. 4 shows some intermediate results. Here, (a) is the original input image; (b) is the image after DPAD; (c) shows the image after polar transformation. After the transformation, the red region is transformed from sector to rectangle. We can get (d) by removing the top N rows of (c). The top N rows show the catheter. We remove other artifacts by deleting the occluded region and finally get (e).

B. Feature Extraction

As shown in Fig. 2, the images from healthy subjects and unhealthy subjects looks quite different in intensity and texture. In this paper we extract intensity feature, Histograms of Oriented Gradients (HOG) [7] and Local Binary Patterns (LBP) [8] bag-of-words (BOW) [9] features to represent the OCT images. HOG captures the edge information, and LBP operator is texture descriptors. Fig. 6 shows the feature extraction process.

- Intensity feature: We resize the image to 32 $\times$ 32 pixels and use the intensity of the resized image as feature directly. In order to reduce dimensionality, we apply

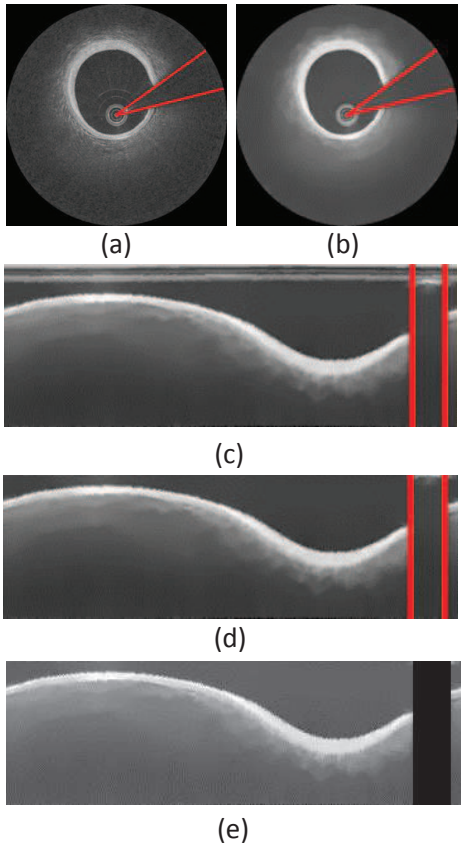

Fig. 4. Preprocessing results. (a) Original image. (b) Remove speckle noise using DPAD. (c) Convert the image to polar coordinates. (d) Remove catheter pixels. (e) Remove other artifacts by deleting the occluded region. Red lines show the occluded region.

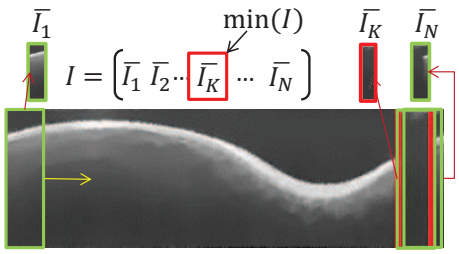

Fig. 5. Process to remove the occluded region. Slide the green box over the image and compute the mean intensity value within the box. The area with least mean intensity value (K-*th* box) is the detected area. The height of the green box is image height, and the width is set to be 30 pixels.

principal component analysis (PCA) [10] and keep the top 95% energy.

- LBP bag-of-words feature: We extract LBP feature and represent each image using LBP bag-of-words (BOW). Bag-of-words is to represent the image using the frequency of the words. We select OCT images which are not used in the evaluation experiment to construct codebook (words) of BOW. The selected images are called codebook images. We compute LBP feature of each image, and use K-means clustering method [11] to get the codebook centres. Here K is set to be 32 empirically.
- HOG bag-of-words feature: We extract HOG feature and quantilizing it using HOG bag-of-words. The same as LBP bag-of-words feature, we compute HOG feature of each codebook image, and use K-means clustering method to get the codebook centres. Here K is set to be 32 empirically.

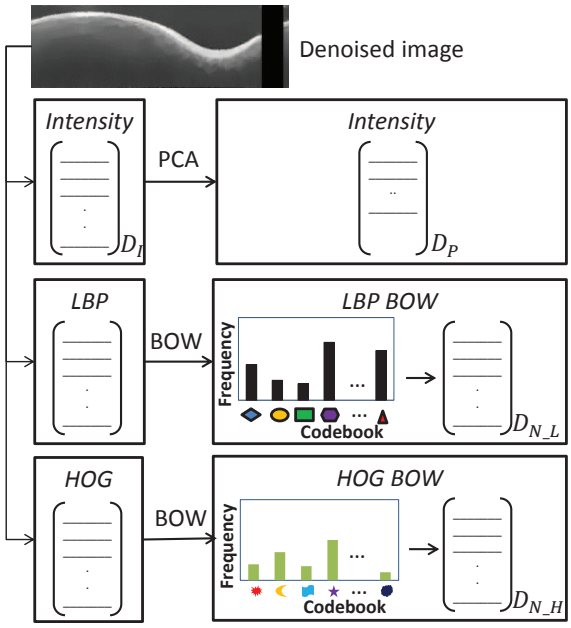

Fig. 6. Feature extraction process. Given the image after preprocessing, we first extract intensity, LBP and HOG feature. For intensity feature, we apply PCA to reduce dimensionality. For LBP and HOG, bag-of-words feature, which represented by the frequency of LBP and HOG words, is computed. Codebooks are constructed using OCT images which are not involved in the learning process.

C. Detection

Linear Support Vector Machine (SVM) [12] is employed to classify the positive and negative samples. Here positive samples are OCT images from unhealthy subjects and negative samples are OCT images from healthy subjects. In this experiment, we use LIBLINEAR package [13] for classification.

III. RESULTS

A. Dataset Construction

We use OCT images from 47 patients for the atherosclerotic heart disease detection system evaluation. The data were collected by Wakayama Medical University. The images were acquired using optical frequency domain imaging (OFDI) equipment (TERUMO LUNAWAVE). This equipment produces high quality frequency domain OCT images at 158 frames per second.

In this experiment, we randomly select 400 frames from the 47 volumes to test the proposed system. They are 200 images from healthy subjects (negative samples) and 200 images from unhealthy subjects (positive samples) which are

TABLE I

MEAN ACCURACY OF THE FOUR-FOLD CROSS-VALIDATION. LBP AND HOG ARE BAG-OF-WORDS FEATURES.

	Mean Accuracy
Intensity	0.85
LBP	0.84
HOG	0.81
Intensity+LBP	0.89
Intensity+HOG	0.87
LBP+HOG	0.86
Intensity+LBP+HOG	**0.90**

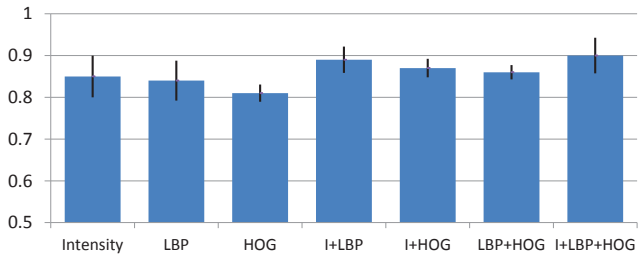

Fig. 7. Four-fold cross-validation results. Blue bar shows mean accuracy value, black bar shows standard deviation.

annotated by experts. All images are resized to 256 $\times$ 256 pixels. We employ a four-fold cross-validation process to evaluate the proposed scheme. The mean value and standard deviation of the four-fold cross-validation are reported.

Fig. 2 shows some images in our dataset. Here (a) and (b) are negative samples, (c) and (d) are positive samples. Specifically, (c) shows image from subject with atherosclerotic plaque, and (d) shows image from subject with ruptured plaque.

B. Experimental Results

A four-fold cross-validation process is used to evaluate the proposed system. The dataset is divided into four subsets with equal size randomly. Noted that our dataset includes 200 positive samples and 200 negative samples, therefore each subset includes 50 positive samples and 50 negative samples. We run the experiment four times and get four accuracy values. For each time, one subset is used as testing set; the others are used as training sets. The mean accuracy value and standard deviation of the four results are reported.

The mean accuracy value and standard deviation are reported in Table I and Fig. 7. Here LBP and HOG are bag-of-words features. We study the single feature (Intensity, LBP, and HOG), as well as feature combinations (I+LBP, I+HOG, LBP+HOG, and I+LBP+HOG). It can be seen that, the accuracy values are higher than 0.80 for all kinds of feature combinations. For single feature, intensity gives the best performance. One possible reason is that intensity keeps the global information better. LBP outperforms HOG, because here texture difference is more important than edge difference. For feature combination, Intensity+LBP+HOG gives best performance, but Intensity + LBP result shows comparable result as the three feature combination result. The standard deviations of the studied features are very small, which indicates that our system is stable.

IV. DISCUSSIONS AND CONCLUSIONS

In this work, an automatic atherosclerotic heart disease detection system is proposed. The system classifies the image from healthy and unhealthy subjects automatically by utilizing texture features. A four-fold cross-validation process is used to evaluate the system and mean accuracy of 0.90 is reported. Different from previous work, our proposed system is fully automated and detects diseased subjects on the image level.

The proposed system could be extended for atherosclerotic grading in future by utilizing lumen and plaque properties. Therefore vessel lumen segmentation and plaque study would be added to our system.

REFERENCES

[1] F. Prati, E. Regar, G. S. Mintz, E. Arbustini, C. Di Mario, I.-K. Jang, T. Akasaka, M. Costa, G. Guagliumi, E. Grube, *et al.*, "Expert review document on methodology, terminology, and clinical applications of optical coherence tomography: physical principles, methodology of image acquisition, and clinical application for assessment of coronary arteries and atherosclerosis," *European heart journal*, vol. 31, no. 4, pp. 401–415, 2010.

[2] F. Prati, G. Guagliumi, G. S. Mintz, M. Costa, E. Regar, T. Akasaka, P. Barlis, G. J. Tearney, I.-K. Jang, E. Arbustini, *et al.*, "Expert review document part 2: methodology, terminology and clinical applications of optical coherence tomography for the assessment of interventional procedures," *European heart journal*, vol. 33, no. 20, pp. 2513–2520, 2012.

[3] S. Tsantis, G. C. Kagadis, K. Katsanos, D. Karnabatidis, G. Bourantas, and G. C. Nikiforidis, "Automatic vessel lumen segmentation and stent strut detection in intravascular optical coherence tomography," *Medical physics*, vol. 39, no. 1, pp. 503–513, 2011.

[4] L. S. Athanasiou, C. V. Bourantas, G. A. Rigas, T. P. Exarchos, A. I. Sakellarios, P. K. Siogkas, M. I. Papafaklis, K. K. Naka, L. K. Michalis, F. Prati, *et al.*, "Fully automated calcium detection using optical coherence tomography," in *Engineering in Medicine and Biology Society (EMBC)*, pp. 1430–1433, IEEE, 2013.

[5] L. Athanasiou, T. Exarchos, K. Naka, L. Michalis, F. Prati, and D. Fotiadis, "Atherosclerotic plaque characterization in optical coherence tomography images," in *Engineering in Medicine and Biology Society (EMBC)*, pp. 4485–4488, IEEE, 2011.

[6] S. Aja-Fernández and C. Alberola-López, "On the estimation of the coefficient of variation for anisotropic diffusion speckle filtering," *IEEE Transactions on Image Processing*, vol. 15, no. 9, pp. 2694–2701, 2006.

[7] N. Dalal and B. Triggs, "Histograms of oriented gradients for human detection," in *Computer Vision and Pattern Recognition*, vol. 1, pp. 886–893, IEEE, 2005.

[8] T. Ojala, M. Pietikainen, and T. Maenpaa, "Multiresolution gray-scale and rotation invariant texture classification with local binary patterns," *IEEE Transactions on Pattern Analysis and Machine Intelligence*, vol. 24, no. 7, pp. 971–987, 2002.

[9] L. Fei-Fei and P. Perona, "A bayesian hierarchical model for learning natural scene categories," in *Computer Vision and Pattern Recognition*, vol. 2, pp. 524–531, IEEE, 2005.

[10] H. Hotelling, "Analysis of a complex of statistical variables into principal components.," *Journal of educational psychology*, vol. 24, no. 6, p. 417, 1933.

[11] C. M. Bishop, *Neural networks for pattern recognition*. Oxford university press, 1995.

[12] C. Cortes and V. Vapnik, "Support-vector networks," *Machine learning*, vol. 20, no. 3, pp. 273–297, 1995.

[13] R.-E. Fan, K.-W. Chang, C.-J. Hsieh, X.-R. Wang, and C.-J. Lin, "Liblinear: A library for large linear classification," *The Journal of Machine Learning Research*, vol. 9, pp. 1871–1874, 2008.